

Received: 2019.04.11  
Accepted: 2019.07.29  
Published: 2019.11.20

# Identification of Potentially Functional CircRNA-miRNA-mRNA Regulatory Network in Gastric Carcinoma using Bioinformatics Analysis

Authors' Contribution:  
Study Design A  
Data Collection B  
Statistical Analysis C  
Data Interpretation D  
Manuscript Preparation E  
Literature Search F  
Funds Collection G

ABCDEF 1 **Guodong Yang**  
BCF 2 **Yujiao Zhang**  
AD 1 **Jiyuan Yang**

1 Department of Oncology, The First People's Hospital Affiliated to Yangtze University, Jingzhou, Hubei, P.R. China  
2 Department of Respiratory Medicine, Huanggang Central Hospital Affiliated to Yangtze University, Huanggang, Hubei, P.R. China

**Corresponding Author:** Jiyuan Yang, e-mail: 18163144297@163.com  
**Source of support:** Departmental sources

**Background:** As all we know, gastric cancer (GC) is a highly aggressive disease. Recently, circular RNA (circRNA) was found to play a vital role in regulation of GC. Some circRNAs could regulate messenger RNA (mRNA) expression by functioning as a microRNA (miRNA) sponge. Nevertheless, the circRNA-miRNA-mRNA regulatory network involved GC rarely has been explored and researched.





**Material/Methods:** All the differentially expressed circRNAs, miRNAs, and mRNA were derived from Gene Expression Omnibus (GEO) microarray data (GSE78092, GSE89143, GSE93415, and GSE54129). GC level 3 miRNA-sequencing data and clinical information were downloaded from The Cancer Genome Atlas (TCGA) database. Furthermore, a circRNA-miRNA-mRNA regulatory network was constructed by Cytoscape (version 3.6.1). Gene Ontology (GO) analysis and Kyoto Encyclopedia of Genes and Genomes (KEGG) pathway revealed the functions and signaling pathways associated with these target genes. Hub genes of protein-protein interaction (PPI) network were identified by STRING database and cytoHubba.

**Results:** The regulatory network consists of 3 circRNAs, 22 miRNAs, and 128 mRNAs. Only 3 miRNAs of the network were consistent with the expression of TCGA and were associated with some clinical features. The results of the functional analysis of 128 mRNAs showed that GO analysis and KEGG pathways of inclusion criteria were 49 and 24, respectively. PPI network and Cytoscape showed that the top 10 hub genes were MYC, CTGF, TGFBR2, TGFBR1, SERPINE1, KRAS, ZEB1, THBS1, CDK6, and TNS1; 4 of which were verified by GEPIA based on TCGA. Highly expressed SERPINE1 had a poor OS (over survival) and DFS (disease-free survival), and TGFBR1 expression increased along with the increase of clinical stages.

**Conclusions:** This study looked at a circRNA-miRNA-mRNA regulatory network associated with GC and explored the potential functions of mRNA in the network, then identified a new molecular marker for prediction, prognosis, and therapeutic targets for clinical patients.

**MeSH Keywords:** **Computational Biology • Biological Markers • Stomach Neoplasms • Gene Expression Profiling**

**Full-text PDF:** <https://www.medscimonit.com/abstract/index/idArt/916902>

 3252  4  11  35



## Background

Gastric cancer (GC) is a disease with very high morbidity and mortality worldwide; it was responsible for over 1 000 000 new cases and 783 000 deaths in 2018, which makes it the fifth most frequently diagnosed cancer and the third leading cause of cancer death [1]. Although there has been significant progress in personalizing treatment for GC, it is still a clinically challenging disease characterized by a lack of effective treatment options and scarcely reliable molecular tools to predict patient outcomes. Compared with other cancer types, the clinical management of GC has not yet achieved the expected benefits from the era of personalized medicine [2]. Almost one third of patients experience recurrence and distant metastasis after undergoing GC surgery [3]. Therefore, the detection of molecular markers for early diagnosis, prognosis, and therapeutic targets of GC has become very urgent.

Most of the human genome is transcribed into non-protein-coding RNA, while protein-coding genome is less than 2% [4]. Circular RNA (circRNA), as one of noncoding RNAs, are derived from the precursor messenger RNA (mRNA) of RNA transcriptase II, consisting of continuous covalently closed loop without the 5'-cap structure and the 3'-poly A tail. Due to this structure, circRNAs are not easily degraded by exonuclease RNase R [5]. In particular, circRNAs are reported to play crucial roles in cancer occurrence, metastasis, and therapy resistance owing to its abundant biological effect on tumor cells including proliferation, apoptosis, and invasion [6]. CircRNAs function primarily as transcriptional and post-transcriptional regulators through various functional mechanisms, such as RNA binding protein (RBP) sponges and protein scaffolds [7], translate proteins [8], RNAP II elongation [9], RNA-RNA interactions [10], and RNA maturation [11]. At present, circRNAs function mainly by adsorbing microRNAs (miRNAs) as miRNA response elements (MRE) based on competing endogenous RNA (ceRNA) hypothesis in GC [12,13]. For instance, augmented expression of circNF1 obviously promotes cell proliferation by sponging miR-16 in GC [14]. Another study reported that has\_circ\_0001461 (termed circFAT1) low expression inhibited GC cell line proliferation by regulating the miR-548g/RUNX1 axis in the cytoplasm and targeting YBX1 in the nucleus, meanwhile, it was correlated with overall survival (OS) of GC patients [15]. In addition, circRNA circPDSS1 has been shown to promote GC progression by sponging miR-186-5p to modulate NEK2 [16].

Although several circRNAs have been identified as participating in the pathogenesis of GC, it is still necessary to conduct a circRNA-miRNA-mRNA regulatory network in GC, to help to advance our understanding of the molecular mechanism of GC. In the present study, we constructed a regulatory network consisting of 3 circRNAs, 22 miRNAs, and 128 mRNAs through

multiple sets of the Gene Expression Omnibus (GEO) database and some online prediction websites, and analyzed the miRNAs and mRNAs in the network using The Cancer Genome Atlas (TCGA) database, the Gene Ontology (GO) analysis, the Kyoto Encyclopedia of Genes and Genomes (KEGG) pathway analysis, and the protein-protein interaction (PPI) network to indirectly understand the potential mechanism of circRNAs in the occurrence and development of GC

## Material and Methods

### Data collection

The microarray data used in the current study were acquired from the GEO database (<http://www.ncbi.nlm.nih.gov/gds/>). The circRNAs expression data were obtained from GSE78092 (3 pairs of primary GC tissue and normal gastric mucosa) and GSE89143 (3 pairs of GC tissue and matched paracancerous tissue). The miRNA and mRNA expression data were respectively derived from GSE93415 (20 pairs of gastric tumor and adjacent healthy gastric mucosa) and GSE54129 (111 tumor samples and 21 normal gastric mucosa). GC level 3 miRNA-sequencing data and clinical information were downloaded from TCGA database (<https://cancergenome.nih.gov/>) on January 07, 2019. A total of 491 samples were included in this study, containing 446 GC samples and 45 matched normal samples. The detailed clinical information included sex, age at diagnosis, grade, T stage, N stage, M stage, and clinical stage, which is shown in Supplementary Table 1.

### Differential expression analysis of circRNAs, miRNAs, and mRNAs

The downloaded platform file(s) and series of matrix file(s) were converted through using the R language software and annotation package. The ID of the corresponding probe name was converted into an international standard name (circRNA symbol). The analysis of differentially expressed RNAs was performed using the limma package based on the Bioconductor package. The criteria for selection of differentially expressed circRNAs (DEcircRNAs) were  $P$ -value  $<0.05$  and  $|\log_2FC| >1$ . Differentially expressed miRNAs (DEmiRNAs) were identified by using GEO2R in dataset GSE93415, as the  $|\log_2FC|$  of most miRNAs is less than 1, we set the criterion that FDR values  $<0.05$  and  $|\log_2FC| >0.5$  were considered significantly. Differentially expressed mRNAs (DEmRNAs) were also identified by using GEO2R in dataset GSE54129, with the criterion that FDR values  $<0.05$  and  $|\log_2FC| >1$  were considered significantly. In addition, miRNA-sequencing data derived from TCGA were processed with edgeR [17], a Bioconductor package based on the R language, to screen differentially expressed miRNAs (TDEmiRNAs) between GC tissue and adjacent normal

tissue. Differentially expressed miRNAs with FDR values  $<0.05$  and  $|\log_2FC| >1$  were considered significantly.

### Construction of the circRNA-miRNA-mRNA regulatory network

According to the results of the differential expression analysis, we first get the intersection of DEcircRNAs between GSE78092 and GSE89143, called IDEcircRNAs. Targeting miRNAs of IDEcircRNAs were predicted via Cancer-Specific CircRNA Database (CSCD) <http://gb.whu.edu.cn/CSCD/> (we called it CPmiRNAs), then we took the intersection of it and DEmiRNAs, which we called ICPDEmiRNAs. Furthermore, we used Perl language to predict respectively their target genes according to downloaded miRNA databases on the 3 target gene prediction website including miRTarBase (<http://mirtarbase.mbc.nctu.edu.tw/>), targetScan (<http://www.targetscan.org>) and miRDB (<http://www.mirdb.org/>). Not all target genes were included, the miRNA target genes that could be found in all 3 databases were used as the final target genes, which were named TmRNA. We took the intersection of it and the DEMRNAs in the same way, and got the final functional genes, which were denominated FmRNAs, therefore, through IDEcircRNAs, ICPDEmiRNAs, and FmRNAs, we constructed the circRNA-miRNA-mRNA regulatory network using Cytoscape.

### Functional enrichment analysis

We firstly converted the gene symbol of FmRNAs in the network into entrezIDs, meanwhile, installing R language packages including “colorspace”, “stringi”, “DOSE”, “clusterProfiler”, and “pathview”. Furthermore, we obtained the outcomes of the GO analysis and the KEGG pathway through R studio and R scripting language, however, not all results were included. We set a criterion that the *P* value of the GO analysis was less than 0.05, besides the *P* value and *q* value of the KEGG analysis were both less than 0.05, and the network diagram of the KEGG pathway containing mRNA was constructed by Cytoscape.

### The analysis of miRNAs and mRNA in the network

We compared ICPDEmiRNAs and TDEmiRNAs by Venn diagram to find the sharing expressed miRNAs, whose expression in tumor tissues and normal tissues was plotted by GraphPad Prism 7, then we analyzed the clinical relevance via SPSS21.0. The hub genes of FmRNAs were screened by PPI and cytoHubba plugin. The medium confidence in the network was 0.400. In addition, their expression, survival prognosis and correlation with clinical stage were identified in GEPIA.

### Statistical analysis

Statistical analysis was performed using SPSS 21.0 (Chicago, IL, USA). Significant differential expression levels of circRNAs were analyzed by R language limma packages and FDR filtering was used for comparative analysis. The *P*-value  $<0.05$  and absolute fold change  $\geq 2.0$  were considered statistically significant. The correlation between miRNA expression and clinical characteristics was tested by chi-square test.

## Results

### Identification of DEcircRNA, DEmiRNAs, DEMRNAs

The integrated analysis of GSE78092 and GSE89143 dataset respectively identified 112 and 54 differentially expressed circRNAs (DEcircRNAs) by R language limma packages, the former included 23 upregulated and 89 downregulated circRNAs, the latter had 8 and 54 (Figure 1). Then, we took the intersection of DEcircRNAs of the 2 datasets, the outcome showed that they didn't have common upregulated circRNAs, while having 3 sharing downregulated circRNAs (IDEcircRNAs) (Figure 2A), which were known as hsa\_circ\_004173, hsa\_circ\_0009076, hsa\_circ\_0028190 (Figure 2B–2D). Besides, we also used GEO2R online analysis on GSE93415 to obtain differentially expressed miRNAs. A total of 344 differentially expressed miRNAs were obtained, 149 of which were downregulated and 195 of which were upregulated (Supplementary Table 2). Similarly, we also did the same analysis on GSE54129, and found 3916 differentially expressed mRNAs, including 1896 upregulated mRNAs and 2020 downregulated mRNAs (Supplementary Table 3).

### Searching for the relationship among circRNA, miRNA, and mRNA

The results of predicted targeting miRNAs on 3 circRNAs shown that hsa\_circ\_0009076 had 48 targeting miRNAs, hsa\_circ\_0028190 had 69, and hsa\_circ\_0041732 had 108. A total of 202 miRNAs were obtained after the removal of the repeatedly targeted miRNAs (Supplementary Table 4). We got 22 common miRNAs (ICPDEmiRNAs) (Supplementary Figure 1A) by taking the intersection of 202 targeting miRNAs and the precious 344 DEmiRNAs. In terms of target gene prediction, we obtained 431 target genes (TmRNAs) of 22 miRNAs (Supplementary Table 5). Finally, we obtained 128 common mRNAs (FmRNAs) (Supplementary Figure 1B) by intersecting the TmRNAs with the previously obtained 3916 DEMRNAs.

### Constructing of circRNA-miRNA-mRNA network.

From the previous data analysis, we got IDEcircRNAs including 3 downregulated circRNAs, 22 ICRDEmiRNAs including 13

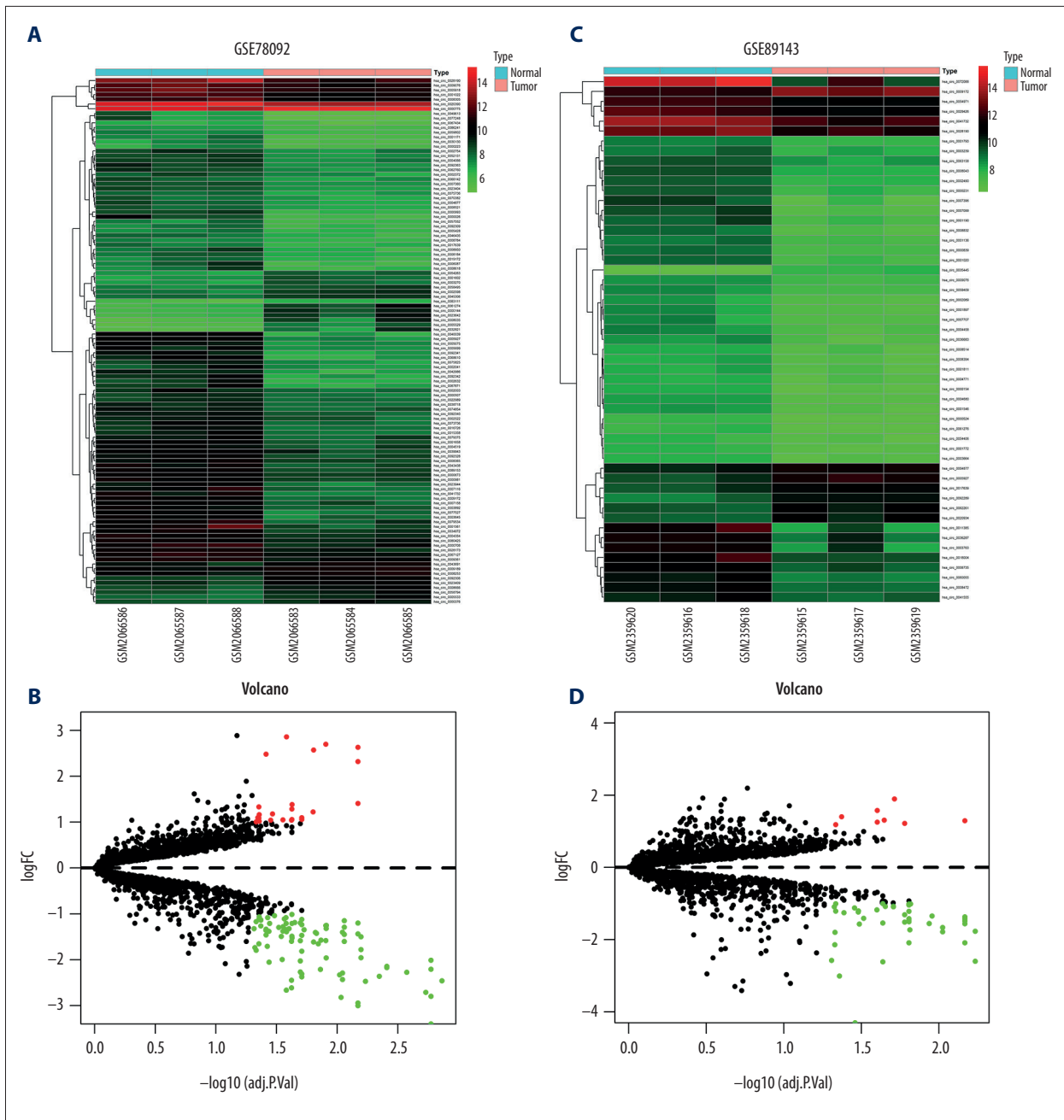


**Figure 1.** Differentially expressed circular RNAs (DEcircRNAs). (A) Heatmap of GSE78092. (B) Volcano plot of GSE78092. (C) Heatmap of GSE89143. (D) Volcano plot of GSE89143.

upregulated, 9 downregulated, 128 FmRNAs including 69 upregulated and 59 downregulated. Then, we use Cytoscape Version3.6.1 soft to describe their relationships in the network, 3 circRNAs had 24 targeted relationship with 22 miRNAs, 22 miRNAs have 139 targeted relationship with 128 DemiRNAs (Figure 3).

**The correlation of clinical characteristics and miRNAs**

In order to further explore clinical correlation of miRNAs in the network, we first got 242 TDEmiRNAs including 178 upregulated and 69 downregulated (Supplementary Table 6, Supplementary Figure 2) in the stomach TCGA database. Compared with the precious 22 ICPDE miRNAs, we got the 3 same expression mode miRNAs. The situation of 3 miRNAs was displayed in Figure 4, then we analyzed their correlation with



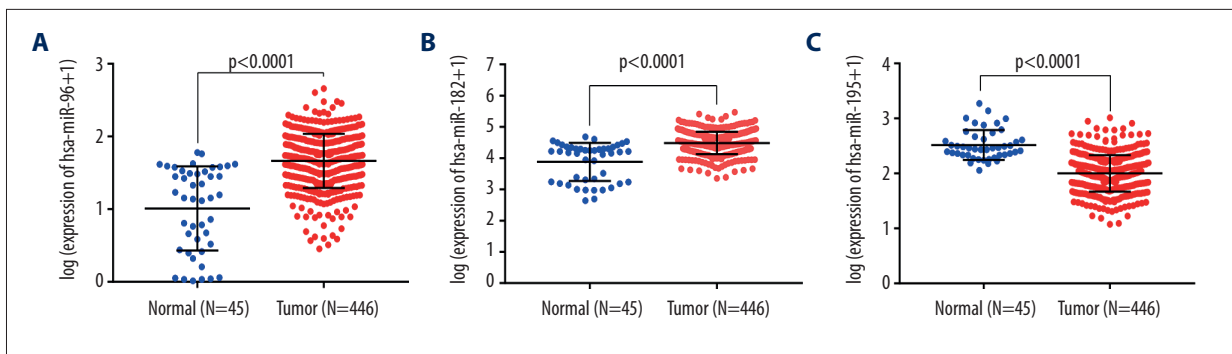


Figure 4. Expression of 3 microRNAs in gastric cancer and normal tissues: (A) hsa-miR-96; (B) hsa-miR-182; (C) hsa-miR-195.

Table 1. Clinical correlation of 3 miRNAs.

Variables	Numbers	hsa-miR-182		$\chi^2$ test P value	hsa-miR-96		$\chi^2$ test P value	hsa-miR-195		$\chi^2$ test P value
		Low expression	High expression		Low expression	High expression		Low expression	High expression	
<b>Gender</b>										
Female	138	66	72	0.495	68	70	0.799	74	64	0.134
Male	235	121	114		119	116		113	122	
<b>Age at diagnosis</b>										
>50	341	176	165	0.062	177	164	0.025	20	12	0.134
≤50	32	11	21		10	22		167	174	
<b>Grade</b>										
G1	6	4	2	0.414	2	4	0.407	4	2	0.414
G2+G3	367	183	184		185	182		183	184	
<b>T stage</b>										
T1+2	97	37	60	0.006	36	61	0.003	56	41	0.405
T3+4	276	150	126		151	125		131	145	
<b>Metastasis</b>										
M0	345	168	177	0.051	170	175	0.244	174	171	0.683
M1	28	199	9		17	11		13	15	
<b>Lymph node status</b>										
N0	120	49	71	0.013	51	69	0.042	70	50	0.029
N1-2	253	138	115		136	117		117	136	
<b>Stage</b>										
I+II	169	81	88	0.438	79	90	0.234	89	80	0.374
III+IV	204	106	98		108	96		98	106	

the clinical characteristics. The results were shown in Table 1: hsa-miR-182 was associated with T stage ( $P=0.006$ ) and N stage ( $P=0.013$ ), hsa-miR-96 was associated with age ( $P=0.025$ ),

T stage ( $P=0.003$ ) and N stage ( $P=0.042$ ), and hsa-mir-195 was associated with N stage ( $P=0.029$ ).

**Table 2.** The results of GO enrichment analysis.

ID	Description	Gene ratio
GO: 0001968	Fibronectin binding	4/122
GO: 0005201	Extracellular matrix structural constituent	7/122
GO: 0019888	Protein phosphatase regulator activity	5/122
GO: 0046332	SMAD binding	5/122
GO: 0019838	Growth factor binding	6/122
GO: 0050431	Transforming growth factor beta binding	3/122
GO: 0019208	Phosphatase regulator activity	5/122
GO: 0001227	Transcriptional repressor activity, RNA polymerase II transcription regulatory region sequence-specific DNA binding	7/122
GO: 0001221	Transcription cofactor binding	3/122
GO: 0004864	Protein phosphatase inhibitor activity	3/122
GO: 0019212	Phosphatase inhibitor activity	3/122
GO: 0072542	Protein phosphatase activator activity	2/122
GO: 0048185	Activin binding	2/122
GO: 0004857	Enzyme inhibitor activity	8/122
GO: 0004674	Protein serine/threonine kinase activity	9/122
GO: 0005024	Transforming growth factor beta-activated receptor activity	2/122
GO: 0030169	Low-density lipoprotein particle binding	2/122
GO: 0070888	E-box binding	3/122
GO: 0019211	Phosphatase activator activity	2/122
GO: 0004675	Transmembrane receptor protein serine/threonine kinase activity	2/122
GO: 0003779	Actin binding	8/122
GO: 0001223	Transcription coactivator binding	2/122
GO: 0030742	GTP-dependent protein binding	2/122
GO: 0019955	Cytokine binding	4/122
GO: 0005518	Collagen binding	3/122
GO: 0017022	Myosin binding	3/122
GO: 0019903	Protein phosphatase binding	4/122
GO: 0005520	Insulin-like growth factor binding	2/122
GO: 0071813	Lipoprotein particle binding	2/122
GO: 0071814	Protein-lipid complex binding	2/122
GO: 0030332	Cyclin binding	2/122
GO: 0035035	Histone acetyltransferase binding	2/122
GO: 0051721	Protein phosphatase 2A binding	2/122
GO: 0019199	Transmembrane receptor protein kinase activity	3/122
GO: 0003713	Transcription coactivator activity	6/122
GO: 1901682	Sulfur compound transmembrane transporter activity	2/122
GO: 0030020	Extracellular matrix structural constituent conferring tensile strength	2/122
GO: 0043531	ADP binding	2/122
GO: 0001078	Transcriptional repressor activity, RNA polymerase II proximal promoter sequence-specific DNA binding	4/122
GO: 0019902	Phosphatase binding	4/122

**Table 2 continued.** The results of GO enrichment analysis.

ID	Description	Gene ratio
GO: 0000982	Transcription factor activity, RNA polymerase II proximal promoter sequence-specific DNA binding	7/122
GO: 0019887	I kinase regulator activity	4/122
GO: 0001228	Transcriptional activator activity, RNA polymerase II transcription regulatory region sequence-specific DNA binding	7/122
GO: 0016706	Oxidoreductase activity, acting on paired donors, with incorporation or reduction of molecular oxygen, 2-oxoglutarate as one donor, and incorporation of one atom each of oxygen into both donors	2/122
GO: 0051018	Protein kinase A binding	2/122
GO: 0045309	Protein phosphorylated amino acid binding	2/122
GO: 0005160	Transforming growth factor beta receptor binding	2/122
GO: 0031625	Ubiquitin protein ligase binding	5/122
GO: 0031490	Chromatin DNA binding	3/122

ID	Bg ratio	p Value	p Adjust	q Value	Gene ID	Count
GO: 0001968	27/17632	3.39E-05	0.012118429	0.011010275	CTGF/FSTL3/THBS1/IGFBP5	4
GO: 0005201	155/17632	0.00010192	0.018243653	0.016575386	FBN2/MUC17/LAMC1/THBS1/TGFBI/COL1A1/COL5A2	7
GO: 0019888	80/17632	0.000232027	0.020766389	0.018867433	PHACTR2/PPP2R5E/PPP1R9B/PPP1R10/CALM2	5
GO: 0046332	80/17632	0.000232027	0.020766389	0.018867433	PRDM16/MYOC/TGFBR1/COL5A2/TGFBR2	5
GO: 0019838	137/17632	0.000381094	0.025089597	0.022795311	CTGF/THBS1/IGFBP5/TGFBR1/COL1A1/TGFBR2	6
GO: 0050431	22/17632	0.000452113	0.025089597	0.022795311	THBS1/TGFBR1/TGFBR2	3
GO: 0019208	94/17632	0.000490579	0.025089597	0.022795311	PHACTR2/PPP2R5E/PPP1R9B/PPP1R10/CALM2	5
GO: 0001227	267/17632	0.002578004	0.098990696	0.089938622	FOXO1/MYC/ZEB1/HEYL/PRDM1/PRRX1/FOXO3	7
GO: 0001221	41/17632	0.002844169	0.098990696	0.089938622	CCNT2/FOXO1/FOXO3	3
GO: 0004864	41/17632	0.002844169	0.098990696	0.089938622	PHACTR2/PPP1R9B/PPP1R10	3
GO: 0019212	44/17632	0.003480829	0.098990696	0.089938622	PHACTR2/PPP1R9B/PPP1R10	3
GO: 0072542	13/17632	0.003523642	0.098990696	0.089938622	PPP2R5E/CALM2	2
GO: 0048185	14/17632	0.004092371	0.098990696	0.089938622	FSTL3/TGFBR1	2
GO: 0004857	371/17632	0.004286672	0.098990696	0.089938622	PHACTR2/TXNIP/SOCS3/PRKAR1A/PPP1R9B/PPP1R10/SERPINH1/SERPINE1	8
GO: 0004674	455/17632	0.004378555	0.098990696	0.089938622	TRPM7/CCNT2/MKNK2/PDIK1L/PRKAA1/CDK6/UHMK1/TGFBR1/TGFBR2	9
GO: 0005024	15/17632	0.004700676	0.098990696	0.089938622	TGFBR1/TGFBR2	2
GO: 0030169	15/17632	0.004700676	0.098990696	0.089938622	LDLR/THBS1	2
GO: 0070888	50/17632	0.004998838	0.099421342	0.090329887	CLOCK/MYC/ZEB1	3
GO: 0019211	16/17632	0.005347991	0.100767416	0.091552872	PPP2R5E/CALM2	2
GO: 0004675	17/17632	0.006033758	0.108004271	0.098127961	TGFBR1/TGFBR2	2
GO: 0003779	421/17632	0.00895487	0.148900927	0.135284877	MYO6/WASF2/TRPM7/PHACTR2/TNS1/MAP1B/CXCR4/PPP1R9B	8
GO: 0001223	21/17632	0.009150336	0.148900927	0.135284877	CCNT2/FOXO1	2
GO: 0030742	22/17632	0.010020159	0.155965948	0.141703845	RAPGEF6/RAB34	2
GO: 0019955	125/17632	0.011123838	0.160730102	0.146032348	THBS1/CXCR4/TGFBR1/TGFBR2	4
GO: 0005518	67/17632	0.011224169	0.160730102	0.146032348	THBS1/TGFBI/SERPINH1	3
GO: 0017022	68/17632	0.011683934	0.160878783	0.146167433	TRPM7/RAB27A/CXCR4	3
GO: 0019903	133/17632	0.013712012	0.181811121	0.16518564	FOXO1/SIRPA/STRN4/PPP1R9B	4
GO: 0005520	28/17632	0.015960482	0.185140606	0.168210665	CTGF/IGFBP5	2



**Table 2 continued.** The results of GO enrichment analysis.

ID	Bg ratio	p Value	p Adjust	q Value	Gene ID	Count
GO: 0071813	28/17632	0.015960482	0.185140606	0.168210665	LDLR/THBS1	2
GO: 0071814	28/17632	0.015960482	0.185140606	0.168210665	LDLR/THBS1	2
GO: 0030332	29/17632	0.017066033	0.185140606	0.168210665	FBXW7/CDK6	2
GO: 0035035	29/17632	0.017066033	0.185140606	0.168210665	MYOCD/CITED2	2
GO: 0051721	29/17632	0.017066033	0.185140606	0.168210665	FOXO1/STRN4	2
GO: 0019199	81/17632	0.018648344	0.196356092	0.178400566	EPHA4/TGFBR1/TGFBR2	3
GO: 0003713	321/17632	0.024230576	0.247844173	0.225180387	PRDM16/RARG/ZEB1/PRRX1/MYOCD/CITED2	6
GO: 1901682	36/17632	0.025665148	0.255225634	0.231886859	SLC35B3/SLC19A3	2
GO: 0030020	37/17632	0.027010862	0.261348336	0.237449679	COL1A1/COL5A2	2
GO: 0043531	39/17632	0.02978569	0.274678286	0.249560689	MYO6/APAF1	2
GO: 0001078	169/17632	0.029923053	0.274678286	0.249560689	FOXO1/HEYL/PRDM1/PRRX1	4
GO: 0019902	178/17632	0.035210199	0.304397033	0.276561844	FOXO1/SIRPA/STRN4/PPP1R9B	4
GO: 0000982	447/17632	0.03582466	0.304397033	0.276561844	KLF5/FOXO1/MYC/HEYL/PRDM1/PRRX1/MYOCD	7
GO: 0019887	180/17632	0.036454143	0.304397033	0.276561844	CCNT2/SOCS3/PRKAR1A/CALM2	4
GO: 0001228	449/17632	0.036561655	0.304397033	0.276561844	KLF5/CLOCK/MYC/HEYL/VEZF1/MYOCD/FOXO3	7
GO: 0016706	47/17632	0.041933365	0.341185106	0.30998588	TET3/P4HA2	2
GO: 0051018	48/17632	0.043562833	0.346566539	0.314875215	WASF2/PRKAR1A	2
GO: 0045309	49/17632	0.045215614	0.351895431	0.319716813	FBXW7/SOCS3	2
GO: 0005160	51/17632	0.04858954	0.352879061	0.320610497	TGFBR1/TGFBR2	2
GO: 0031625	286/17632	0.048696742	0.352879061	0.320610497	FOXO1/FBXW7/TXNIP/CXCR4/PRKAR1A	5
GO: 0031490	119/17632	0.049642361	0.352879061	0.320610497	CLOCK/PRDM1/FOXO3	3

## GO and KEGG analysis of FmRNAs

128 FmRNAs were used to detect the potential functions of circRNA, including GO enrichment analysis and KEGG pathway analysis. In the GO analysis, including biological process, cellular component and molecular function, we obtained 49 results, which were shown in Table 2. In KEGG pathway analysis, we got 24 results, which were shown in Table 3. The dotplot showed the results of the top 20 GO analysis results with *P* value from small to large, as well as the results of KEGG pathway, most of which were related to the density of tumor (Figure 5A, 5B). In addition, we also constructed the network diagram of the relationship between KEGG pathway and each mRNA (Figure 5C). In the tumor-associated signaling pathway, KEGG analysis showed that the PI3K-Akt signaling pathway contained the most genes (PRKAA1/MYC/CDK6/KRAS/LAMC1/THBS1/COL1A1/PPP2R5E/FOXO3) (Supplementary Figure 3A), and the p53 signaling pathway including PERP/APAF1/CDK6/SESN2/THBS1/SERPINE1 had the smallest *P*-value (Supplementary Figure 3B), which showed the most significance. The 2 signaling pathways became the focus of our observation.

## Screening of hub genes

In order to further find the hub genes of 128 FmRNAs in the network, STRING database (<http://string-db.org>), Cytoscape and its plugin (cytoHubba) were applied, and the results showed that 86 genes were related to each other (Figure 6A). According to cytoHubba plugin's MCC ranking, the top 10 hub genes were MYC (v-myc avian myelocytomatosis viral oncogene homolog), CTGF (connective tissue growth factor), TGFBR2 (TGF-beta receptor type-2), TGFBR1 (TGF-beta receptor type-1), SERPINE1 (plasminogen activator inhibitor 1), KRAS (Kirsten rat sarcoma viral oncogene homolog), ZEB1 (zinc finger E-box-binding homeobox 1), THBS 1 (thrombospondin-1), CDK6 (cyclin-dependent kinase 6), TNS1 (tensin-1) (Figure 6B, Table 4). The expression of all the 10 genes was verified on the GEPIA, and it was found that MYC, TGFBR1, SERPINE1, and CDK6 showed statistically significant differences in expression (Figure 7). In addition, we also found that highly expressed SERPINE1 had a poor OS and disease-free survival (DFS), and TGFBR1 expression increased along with the increase of clinical stages (Figure 8) [18].

**Table 3.** The results of KEGG pathway analysis.

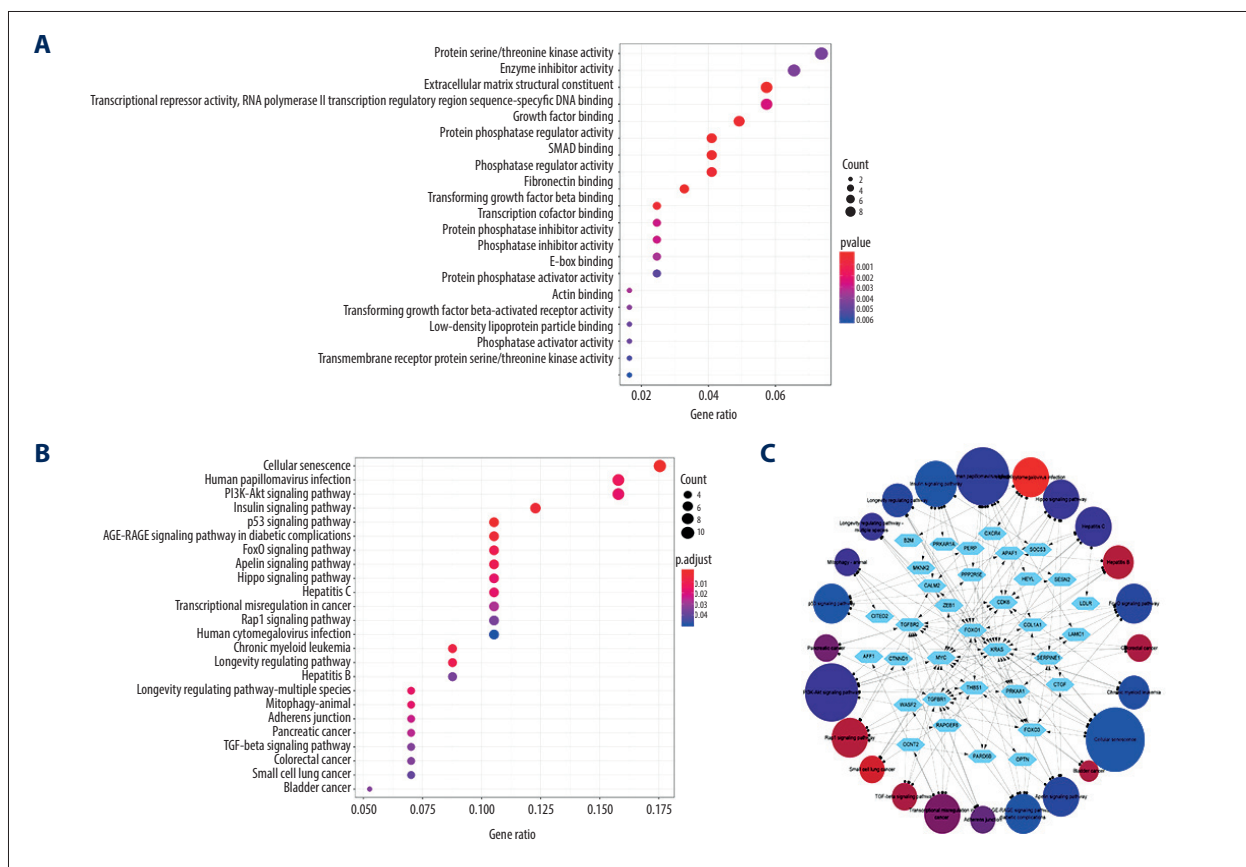
ID	Description	Gene ratio	Bg ratio	p Value
hsa04218	Cellular senescence	10/57	160/7466	2.80E-07
hsa04115	p53 signaling pathway	6/57	72/7466	1.60E-05
hsa04910	Insulin signaling pathway	7/57	137/7466	7.39E-05
hsa04933	AGE-RAGE signaling pathway in diabetic complications	6/57	99/7466	9.81E-05
hsa05220	Chronic myeloid leukemia	5/57	76/7466	0.000265202
hsa04068	FoxO signaling pathway	6/57	132/7466	0.000472257
hsa04211	Longevity regulating pathway	6/57	89/7466	0.000552582
hsa04371	Apelin signaling pathway	6/57	137/7466	0.000575675
hsa05165	Human papillomavirus infection	9/57	330/7466	0.000794412
hsa04390	Hippo signaling pathway	6/57	154/7466	0.001064365
hsa05160	Hepatitis C	6/57	155/7466	0.001100757
hsa04213	Longevity regulating pathway - multiple species	6/57	62/7466	0.00122559
hsa04151	PI3K-Akt signaling pathway	9/57	354/7466	0.0013066
hsa04137	Mitophagy – animal	4/57	65/7466	0.001462455
hsa04520	Adherens junction	4/57	72/7466	0.002136126
hsa05212	Pancreatic cancer	4/57	75/7466	0.002481334
hsa05202	Transcriptional misregulation in cancer	6/57	186/7466	0.002786785
hsa05219	Bladder cancer	3/57	41/7466	0.003662102
hsa04350	TGF-beta signaling pathway	4/57	85/7466	0.003907022
hsa05210	Colorectal cancer	4/57	86/7466	0.004074595
hsa04015	Rap1 signaling pathway	6/57	206/7466	0.004611998
hsa05161	Hepatitis B	5/57	144/7466	0.004659537
hsa05222	Small cell lung cancer	4/57	93/7466	0.005385847
hsa05163	Human cytomegalovirus infection	6/57	225/7466	0.007051458

ID	p. Adjust	q Value	Gene ID	Count
hsa04218	4.68E-05	3.51E-05	TRPM7/FOXO1/MYC/CDK6/KRAS/TGFBR1/TGFBR2/SERPINE1/CALM2/FOXO3	10
hsa04115	0.001338182	0.001003742	PERP/APAF1/CDK6/SESN2/THBS1/SERPINE1	6
hsa04910	0.004095217	0.003071736	FOXO1/MKNK2/PRKAA1/KRAS/SOCS3/PRKAR1A/CALM2	7
hsa04933	0.004095217	0.003071736	FOXO1/KRAS/TGFBR1/COL1A1/TGFBR2/SERPINE1	6
hsa05220	0.008857732	0.006643997	MYC/CDK6/KRAS/TGFBR1/TGFBR2	5
hsa04068	0.012017218	0.00901386	FOXO1/PRKAA1/KRAS/TGFBR1/TGFBR2/FOXO3	6
hsa04211	0.012017218	0.00901386	FOXO1/PRKAA1/KRAS/SESN2/FOXO3	5
hsa04371	0.012017218	0.00901386	PRKAA1/KRAS/CTGF/TGFBR1/SERPINE1/CALM2	6
hsa05165	0.014740748	0.011056723	FOXO1/PARD6B/CDK6/KRAS/HEYL/LAMC1/THBS1/COL1A1/PPP2R5E	9
hsa04390	0.016711491	0.012534935	PARD6B/MYC/CTGF/TGFBR1/TGFBR2/SERPINE1	6
hsa05160	0.016711491	0.012534935	LDLR/APAF1/MYC/CDK6/KRAS/SOCS3	6
hsa04213	0.016784782	0.012589909	FOXO1/PRKAA1/KRAS/FOXO3	4
hsa04151	0.016784782	0.012589909	PRKAA1/MYC/CDK6/KRAS/LAMC1/THBS1/COL1A1/PPP2R5E/FOXO3	9
hsa04137	0.017444997	0.013085122	OPTN/KRAS/CITED2/FOXO3	4

**Table 3 continued.** The results of KEGG pathway analysis.

ID	p. Adjust	q Value	Gene ID	Count
hsa04520	0.023782202	0.017838526	WASF2/CTNND1/TGFBR1/TGFBR2	4
hsa05212	0.025898925	0.019426234	CDK6/KRAS/TGFBR1/TGFBR2	4
hsa05202	0.027376065	0.020534206	CCNT2/FOXO1/MYC/ZEB1/AFF1/TGFBR2	6
hsa05219	0.033976167	0.025484802	MYC/KRAS/THBS1	3
hsa04350	0.03402287	0.025519833	MYC/THBS1/TGFBR1/TGFBR2	4
hsa05210	0.03402287	0.025519833	MYC/KRAS/TGFBR1/TGFBR2	4
hsa04015	0.03537012	0.026530377	PARD6B/RAPGEF6/CTNND1/KRAS/THBS1/CALM2	6
hsa05161	0.03537012	0.026530377	APAF1/MYC/CDK6/KRAS/TGFBR1	5
hsa05222	0.03910593	0.029332528	APAF1/MYC/CDK6/LAMC1	4
hsa05163	0.049066392	0.03680366	B2M/MYC/CDK6/KRAS/CXCR4/CALM2	6



**Figure 5.** Functional analysis of 128 DEmi-mRNAs. **(A)** The dotplot of top 20 GO analysis. **(B)** The dotplot of KEGG pathway. **(C)** The network diagram between KEGG pathways and mRNA. The larger the circle, the more genes it contained; conversely, the smaller the circle, the fewer genes it contained. The color of the circle is correlated with the *P*-value. The smaller the *P*-value is, the closer it is to the red value. The larger the *P*-value is, the closer it is to the blue value. DE – differentially expressed; mi – micro; m – messenger; GO – Gene Ontology; KEGG – Kyoto Encyclopedia of Genes and Genomes.

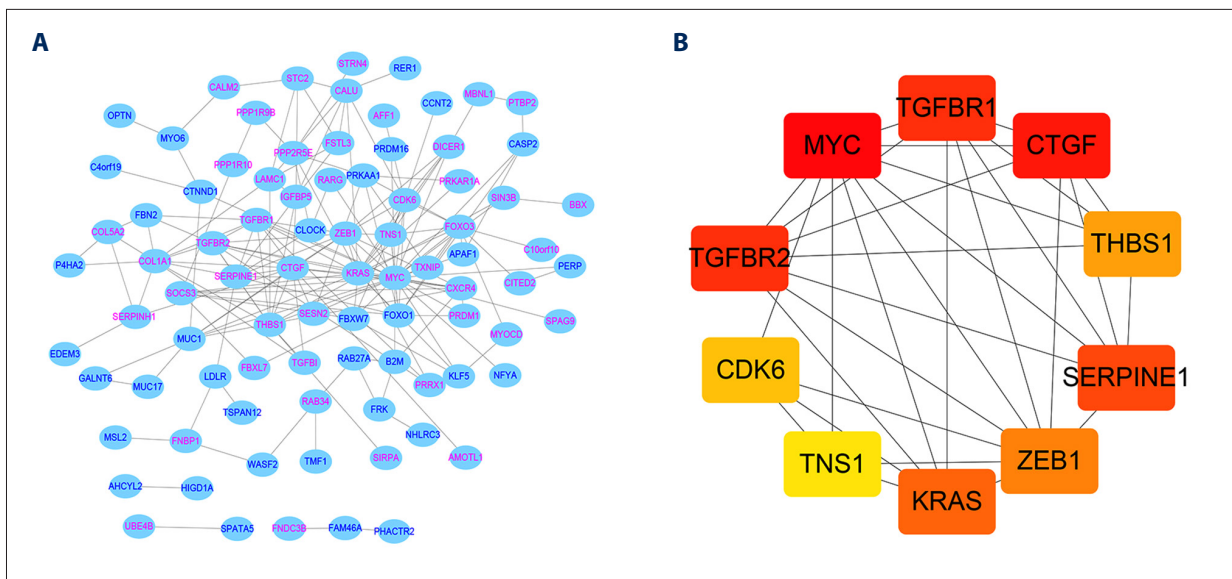


**Figure 6.** (A) PPI network diagram of 86 DEmi-mRNAs. (B) The network diagram of top 10 hub genes. PPI – protein-protein interaction; DE – differentially expressed; miRNA – microRNA; mRNA – messenger RNA.

**Table 4.** The rank of hub genes via various of situations.

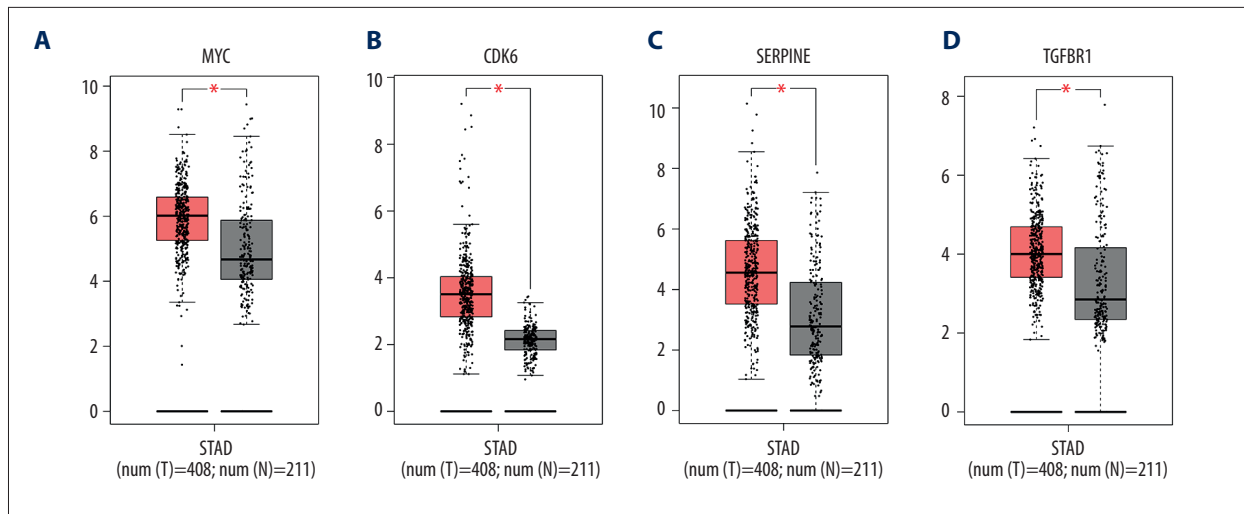
Node name	MCC	DMNC	MNC	Degree	EPC	Bottle neck	Ec centrivity	Close-ness	Radia- lity	Between- ness	Stress	Clustering coefficient
MYC	609	0.24794	25	30	36.302	49	0.22965	50.91667	5.72361	2930.436	6766	0.13563
CTGF	401	0.37042	13	14	35.37	8	0.18372	40.61667	5.33497	676.2413	2134	0.31868
TGFB2	396	0.49882	10	10	34.088	3	0.18372	38.03333	5.25253	183.2476	1158	0.55556
TGFB1	396	0.49882	10	10	33.892	1	0.18372	38.03333	5.25253	183.2476	1158	0.55556
SERPINE1	370	0.5012	9	11	34.56	8	0.18372	39.45	5.34675	868.6996	2280	0.38182
KRAS	322	0.36053	15	17	36.072	16	0.18372	42.76667	5.39386	828.0731	2704	0.26471
ZEB1	318	0.45368	12	12	35.42	8	0.18372	39.2	5.28787	194.055	870	0.4697
THBS1	259	0.41901	10	11	33.93	6	0.18372	38.61667	5.26431	402.2999	1202	0.38182
CDK6	250	0.47733	9	11	33.692	3	0.18372	38.26667	5.20543	428.6176	1188	0.36364
TNS1	240	0.62199	7	7	32.135	1	0.18372	35.18333	5.07588	8.55088	56	0.80952
COL1A1	142	0.32239	11	11	33.115	4	0.1531	34.35	4.85212	350.8601	1722	0.34545
FOXO1	134	0.31924	10	10	33.841	4	0.18372	37.95	5.24076	203.7761	800	0.35556
FOXO3	131	0.4082	8	11	32.054	2	0.18372	36.85	5.09943	398.0874	1268	0.25455
DICER1	121	0.64826	5	6	29.184	2	0.18372	34.18333	5.02877	157.1734	434	0.66667
CXCR4	58	0.37904	8	8	32.284	11	0.18372	36.86667	5.2172	178.6964	600	0.46429
MUC1	52	0.47549	6	8	30.378	5	0.18372	36.43333	5.1701	366.1695	864	0.39286
IGFBP5	32	0.36588	7	7	28.18	1	0.1531	32.31667	4.82856	193.0638	622	0.47619
LAMC1	28	0.38039	6	6	26.728	1	0.1531	30.46667	4.67546	88.60129	278	0.53333
CALU	27	0.56839	4	7	27.046	7	0.1531	32.88333	4.87567	368.5913	1006	0.33333

**Table 4 continued.** The rank of hub genes via various of situations.

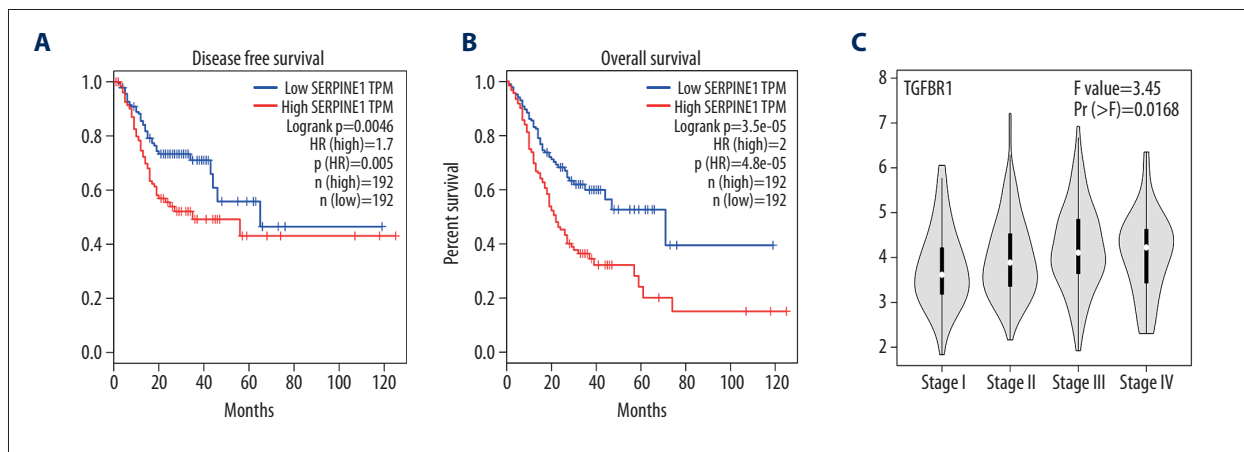
Node name	MCC	DMNC	MNC	Degree	EPC	Bottle neck	Ec centrality	Close-ness	Radia- lity	Between- ness	Stress	Clustering coefficient
STC2	25	0.56839	4	5	21.431	2	0.13123	27.22619	4.34571	112.2128	258	0.6
FSTL3	24	0.56839	4	4	21.367	1	0.13123	26.34286	4.28682	0	0	1
SOCS3	21	0.38039	6	7	29.643	3	0.18372	34.51667	5.02877	250.4977	792	0.38095
FBXW7	20	0.38039	6	6	29.119	1	0.18372	34.18333	5.02877	77.23846	304	0.53333
FBN2	8	0.37893	4	4	23.641	2	0.1531	27.75	4.48703	26.03518	280	0.66667
KLF5	7	0.46346	3	4	24.062	2	0.18372	32.68333	4.96989	59.30048	238	0.5
PRKAA1	7	0.30898	3	6	25.204	1	0.1531	30.03333	4.6048	61.26671	174	0.13333
PRRX1	6	0.46346	3	3	23.368	1	0.1531	27.36667	4.48703	0	0	1
TGFBI	6	0.46346	3	3	23.103	1	0.1531	28.15	4.53414	0	0	1
COL5A2	6	0.2842	4	4	19.627	1	0.13123	24.70952	3.9924	5	10	0.5
PPP2R5E	5	0	1	5	19.69	3	0.1531	30.61667	4.69902	302.8195	790	0
CASP2	5	0.30898	3	4	20.746	2	0.18372	31.93333	4.88745	143.4932	330	0.33333
SERPINH1	5	0.30898	3	4	20.532	2	0.1531	28.4	4.52236	171.9268	490	0.33333
TXNIP	4	0.30898	3	3	20.773	2	0.18372	32.1	4.93456	12.23252	76	0.66667
PRDM1	4	0.30898	3	3	22.727	1	0.18372	31.1	4.85212	0.68182	4	0.66667
B2M	4	0.30779	2	4	18.355	7	0.18372	32.53333	4.96989	716.2094	1514	0.33333
CTNND1	4	0.30779	2	4	18.921	5	0.18372	32.68333	4.95811	480.2316	832	0.16667
APAF1	4	0.30898	3	3	20.821	1	0.18372	31.76667	4.89922	4.66667	16	0.66667
SIN3B	3	0.30779	2	3	18.56	2	0.18372	32.26667	4.95811	154	238	0.33333
FNBP1	3	0	1	3	4.766	3	0.1531	22.36667	3.81574	277.7906	550	0
LDLR	3	0	1	3	11.833	5	0.18372	27.81667	4.58125	537.7906	1026	0
FRK	3	0.30779	2	3	7.811	2	0.18372	24.4	4.15727	154	298	0.33333
MYO6	3	0	1	3	8.446	3	0.1531	24.88333	4.19261	218.1825	368	0
SESN2	3	0.30779	2	3	21.783	1	0.18372	32.85	5.01699	34.11001	178	0.33333
RAB27A	3	0.30779	2	3	8.435	4	0.18372	24.86667	4.20438	326.2094	692	0.33333
RAB34	3	0	1	3	4.339	3	0.1531	20.68333	3.43888	210.7381	444	0
CLOCK	3	0	1	3	16.66	1	0.1531	28.1	4.58125	65.63025	158	0
PERP	2	0	1	2	12.381	2	0.18372	30.6	4.84034	43.91725	162	0
CALM2	2	0	1	2	8.433	1	0.13123	22.04286	3.76863	29.95094	44	0
RARG	2	0	1	2	14.151	2	0.18372	30.93333	4.87567	28.30952	88	0
WASF2	2	0	1	2	3.067	1	0.13123	18.80952	3.06202	38.52872	68	0
MBNL1	2	0	1	2	10.944	1	0.1531	24.3	4.15727	10.72727	40	0
MYOCD	2	0	1	2	14.687	1	0.1531	25.3	4.23971	2.05556	8	0
FAM46A	2	0	1	2	1.568	3	0.03488	2	0.12209	2	2	0

Table 4 continued. The rank of hub genes via various of situations.

Node name	MCC	DMNC	MNC Degree	EPC	Bottle neck	Ec centrality	Close-ness	Radia- lity	Between- ness	Stress	Clustering coefficient	
PRKAR1A	2	0	1	2	16.389	1	0.1531	27.86667	4.53414	4.43252	46	0
CITED2	2	0	1	2	12.229	1	0.1531	25.05	4.21616	3.06667	8	0
PPP1R10	2	0	1	2	11.151	1	0.1531	24.55	4.18083	27.70586	98	0
PPP1R9B	2	0	1	2	8.77	1	0.13123	22.55952	3.8393	7	8	0
PTBP2	2	0	1	2	8.932	1	0.1531	23.3	4.01595	3.55385	8	0
P4HA2	2	0.30779	2	2	13.847	1	0.13123	23.54286	3.95707	0	0	1
GALNT6	2	0.30779	2	2	11.642	1	0.1531	24.96667	4.27504	0	0	1
FBXL7	2	0.30779	2	2	15.652	1	0.1531	24.63333	4.19261	0	0	1
MUC17	2	0.30779	2	2	11.691	1	0.1531	24.96667	4.27504	0	0	1
RER1	1	0	1	1	8.885	1	0.13123	22.69286	3.96884	0	0	0
AMOTL1	1	0	1	1	12.027	1	0.1531	26.06667	4.42815	0	0	0
SPAG9	1	0	1	1	10.867	1	0.18372	29.93333	4.81679	0	0	0
SIRPA	1	0	1	1	10.606	1	0.1531	25.31667	4.35748	0	0	0
AHCYL2	1	0	1	1	1.322	1	0.02326	1	0.06977	0	0	0
HIGD1A	1	0	1	1	1.322	1	0.02326	1	0.06977	0	0	0
PHACTR2	1	0	1	1	1.374	1	0.01744	1.5	0.10465	0	0	0
MSL2	1	0	1	1	2.175	1	0.13123	17.24286	2.90891	0	0	0
AFF1	1	0	1	1	10.166	1	0.1531	25.1	4.2986	0	0	0
TMF1	1	0	1	1	2.402	1	0.13123	16.14524	2.53205	0	0	0
C4orf19	1	0	1	1	6.234	1	0.1531	22.86667	4.05128	0	0	0
STRN4	1	0	1	1	6.291	1	0.13123	21.64286	3.79219	0	0	0
BBX	1	0	1	1	6.08	1	0.1531	22.75	4.05128	0	0	0
SPATA5	1	0	1	1	1.289	1	0.02326	1	0.06977	0	0	0
UBE4B	1	0	1	1	1.289	1	0.02326	1	0.06977	0	0	0
PRDM16	1	0	1	1	11.749	1	0.18372	29.93333	4.81679	0	0	0
C10orf10	1	0	1	1	9.952	1	0.1531	24.38333	4.19261	0	0	0
OPTN	1	0	1	1	3.585	1	0.13123	18.7619	3.28578	0	0	0
TSPAN12	1	0	1	1	4.562	1	0.1531	20.43333	3.67442	0	0	0
FNDC3B	1	0	1	1	1.358	1	0.01744	1.5	0.10465	0	0	0
EDEM3	1	0	1	1	7.224	1	0.13123	20.55952	3.61553	0	0	0
CCNT2	1	0	1	1	10.511	1	0.1531	25.1	4.2986	0	0	0
NHLRC3	1	0	1	1	3.536	1	0.1531	18.5	3.25045	0	0	0
NFYA	1	0	1	1	11.172	1	0.18372	29.93333	4.81679	0	0	0



**Figure 7.** Four hub genes expression in GEPIA; (A) MYC, (B) CDK6, (C) SERPINE, (D) TGFBF1.



**Figure 8.** (A) Disease-free survival of SERPINE; (B) overall survival of SERPINE. (C) Relationship between clinical stage and TGFBF1 expression.

## Discussion

Although the levels of diagnosis and treatment of GC is constantly improving, GC is still a high-risk disease, and a large part of its potential occurrence and development mechanism is still unclear. Prior to this, many studies on the pathogenesis of GC have been presented, but mainly focusing on genes encoding proteins. Since non-coding protein RNAs have appeared in everyone's field of vision and have been found to have specific regulatory functions, researchers have been investigating more and more non-coding RNAs, especially circRNAs. In this study, we discovered a few new circRNAs that target the regulation of downstream genes through sponge-adsorbed miRNAs. We also performed functional analysis of these target genes to understand the potential functions of these circRNAs.

In our study, we obtained a network of 3 circRNAs, 22 miRNAs, and 128 mRNAs using the GEO datasets. In addition, we found

that on the CSCD website that hsa\_circ\_0009076 was composed of the 29<sup>th</sup> and 30<sup>th</sup> exons of the reverse transcript of the gene NRDC (location: 1p32.3, exon count: 35), hsa\_circ\_0028190 was composed of the 6<sup>th</sup>–11<sup>th</sup> exons of the reverse transcript of the gene ANAPC7 (location: 12q24.11, exon count: 13), and hsa\_circ\_0041732 was composed of the 8<sup>th</sup> exons of the forward transcript of the gene FAM64A (location: 17p13.2, exon count: 16). The 3 circRNAs have not been reported previous in the literature. We named hsa\_circ\_0009076, hsa\_circ\_0028190, and hsa\_circ\_0041732 respectively as circNRDC, circANAPC7, and circFAM64A. In the future, more experiments will be needed to verify the expression of these circRNAs and their effects on the proliferation, apoptosis, invasion, and metastasis of GC cells.

In order to explore the indirect mechanism of circRNAs on GC, miRNAs and mRNAs of circRNAs downstream in the regulatory network were further analyzed. We validated the 22 differentially expressed miRNAs in TCGA database and found that the

3 miRNAs had the same expression (has-miR-96, has-miR-182, and has-miR-195). The correlation with clinical features by chi-square test demonstrated that hsa-mir-182 was associated with T stage and N stage, hsa-mir-96 was associated with age, T stage, and N stage, and hsa-mir-195 was associated with N stage, although only 3 of the 22 miRNAs have been confirmed, which may be due to different sample and statistical methods; more experiments are needed to verify our results. Hsa-miR-96-5p has been reported in many studies, for example, miR-96 was successfully shown to increase expression in GC compared to normal or adenoma samples and was further validated with real-time quantitative polymerase chain reaction (RT-qPCR) in 77 samples [19]. Hsa-miR-96 was shown to be upregulated in tumor tissues and HepG2 cells, and to promote tumorigenesis and progression by inhibiting FOXO1 and activating of AKT/GSK-3 $\beta$ / $\beta$ -catenin signaling pathway in hepatocellular carcinoma [20]. In addition, hsa-miR-96 accelerates invasion and migration of bladder cancer through epithelial-mesenchymal transition in response to transforming growth factor- $\beta$ 1 [21]. One circRNA can adsorb multiple miRNAs, meanwhile, one miRNA can also be adsorbed by multiple circRNAs. In addition, we found that mir-182-5p in our network could be adsorbed by hsa\_circ\_0041732. Sun et al. showed that high expression of circ-SFMBT2 was related to the advanced progression of GC. The functional mechanism experiment showed that circ-SFMBT2 could regulate CREB1 by sponging mir-182-5p to promote the progression of GC [22]. Li et al. showed that miR-182-5p had a higher expressed level through comparison between GC tissue and normal tissue, and improved the viability, mitosis, migration, and invasion ability of human GC cells by downregulating RAB27A [23]. Wang et al. reported that expression levels of miR-195-5p and bFGF showed negative correlation in human GC tissues and miRNA-195 suppressed human GC by binding basic fibroblast growth factor [24]. Ye et al. demonstrated that miR-195 overexpression restrained invasion, migration, and proliferation of GC cells *in vitro* and enhanced the chemotherapy sensitivity of cisplatin in GC cells, furthermore, benefiting survival prognosis of GC patients [25]. These studies confirmed that the expression of the 3 miRNAs in our network was indeed involved in the occurrence and progression of GC.

Among KEGG tumor-related signaling pathways, PI3K-Akt signaling pathway contains the largest number of genes (PRKAA1/MYC/CDK6/KRAS/LAMC1/THBS1/COL1A1/PPP2R5E/FOXO3), while p53 signaling pathway (PERP/APAF1/CDK6/SESN2/THBS1/SERPINE1) has the smallest *P* value. We focused on these 2 signaling pathways. The PI3K/Akt signaling pathway functions as a vital intermediary to facilitate various cellular and physiological processes, including the cell cycle, cellular growth, differentiation, survival, apoptosis, metabolism, angiogenesis, and migration [26]. Accumulating evidence has displayed that crucial epigenetic modifiers are directly or indirectly

regulated by PI3K/AKT signaling and involved in oncogenesis of PI3K cascade in cancers [27]. The core of p53 signaling pathway is p53, which functions as safeguarding the integrity of the genome. Activation of p53 affects apoptosis, cell cycle arrest, angiogenesis, DNA repair, and metastasis by mainly regulating downstream targeting genes [28]. Wei et al. showed that overexpression of lncRNA MEG3 could increase the expression of p53, then its conclusion demonstrated that lncRNA MEG3 restrain proliferation and metastasis of GC via p53 signaling pathway [29]. In our regulatory network, both THBS1 and CDK6 are involved in the regulation of PI3K-Akt and p53 signaling pathways. THBS1 was the first member of extracellular matrix (ECM) proteins family, which acts as an angiogenesis inhibitor and regulates tumor cell adhesion, invasion, migration, proliferation, apoptosis, and tumor immunity [30,31]. CDK6 function cell-cycle progression, transcription, tissue homeostasis and differentiation as one member of cyclin-dependent kinases [32]. A recent study found that the inhibition of hsa\_circ\_0081143 reduced GC cells invasion ability, viability, and increased the sensitivity of GC cells to cisplatin (DDP) *in vitro* act as an endogenous sponge adsorption by directly binding to miR-646 and efficiently inverting the inhibition of CDK6 [33].

The 4 of top 10 hub genes (THBS1, CDK6, SERPINE1, TGFBR1) in the PPI network were consistent with the expression of GEPIA. Their survival analysis and clinical stage correlated with the expression were further explored. It was found that highly expressed SERPINE1 had a poor prognosis, and the expression of TGFBR1 was positively correlated with clinical stage. SERPINE1 encodes a member of the serine proteinase inhibitor (serpin) superfamily, which is the principal inhibitor of tissue plasminogen activator (tPA) and urokinase (uPA). Overexpression of uPA/uPAR and SERPINE1 promotes tumor cell invasion and migration, playing an important role in metastasis development, conferring poor prognosis. In addition, both uPA/uPAR and SERPINE1 are directly associated with the induction of the acquisition of stem cell properties, epithelial-to-mesenchymal transition and resistance to antitumor agents [34]. The protein encoded by TGFBR1, as a serine/threonine protein kinase, forms a heteromeric complex with type II TGF-beta receptors when bound to TGF-beta, transducing the TGF-beta signal from the cell surface to the cytoplasm, which participated in the regulation of various cell physiology and pathological processes, including adhesion, motility, differentiation, division and apoptosis, and plays a vital role in tumor invasion and metastasis by mediating epithelial-to-mesenchymal transition (EMT) [35]. So in our regulatory network, we found 4 important circRNA-miRNA-mRNA axis including hsa\_circ\_0041732/hsa-mir-182-5p/THBS1, hsa\_circ\_0028190/hsa-mir-4291/CDK6, hsa\_circ\_0009076/hsa-mir-143-3p/SERPINE1, and hsa\_circ\_0028190/hsa-mir-140-5p/TGFBR1 about the 3



circRNAs. In future studies, more experiments are expected to verify this possible ceRNA mechanism in GC.

## Conclusions

Although there are some studies on circRNA in GC, the number and methods of research are different. In this study, we constructed a circRNA-miRNA-mRNA regulatory network including 3 important circRNAs (hsa\_circ\_0009076, hsa\_circ\_0028190, and hsa\_circ\_0041732) through multiple GEO databases and TCGA database and performed functional enrichment analysis on these final target genes for understanding the potential

functional mechanisms of circRNA. Of course, it is more important to combine basic experiments with clinical data to further explore the feasibility of these circRNAs, so as to provide new molecular marker of prediction, prognosis, and therapeutic targets for clinical patients.

## Acknowledgements

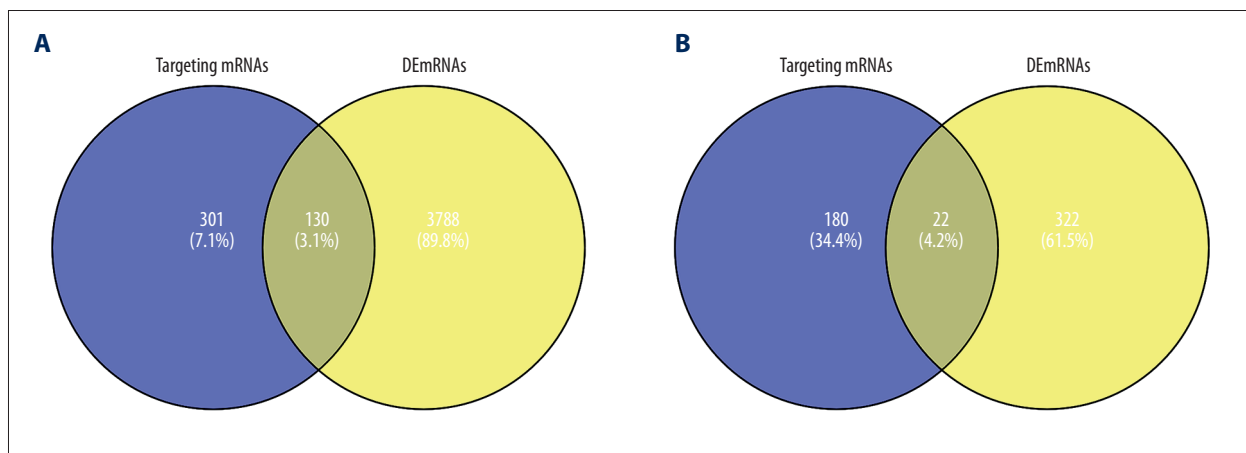
We thank Zhaowu Ma for the technical advice.

## Conflict of interests

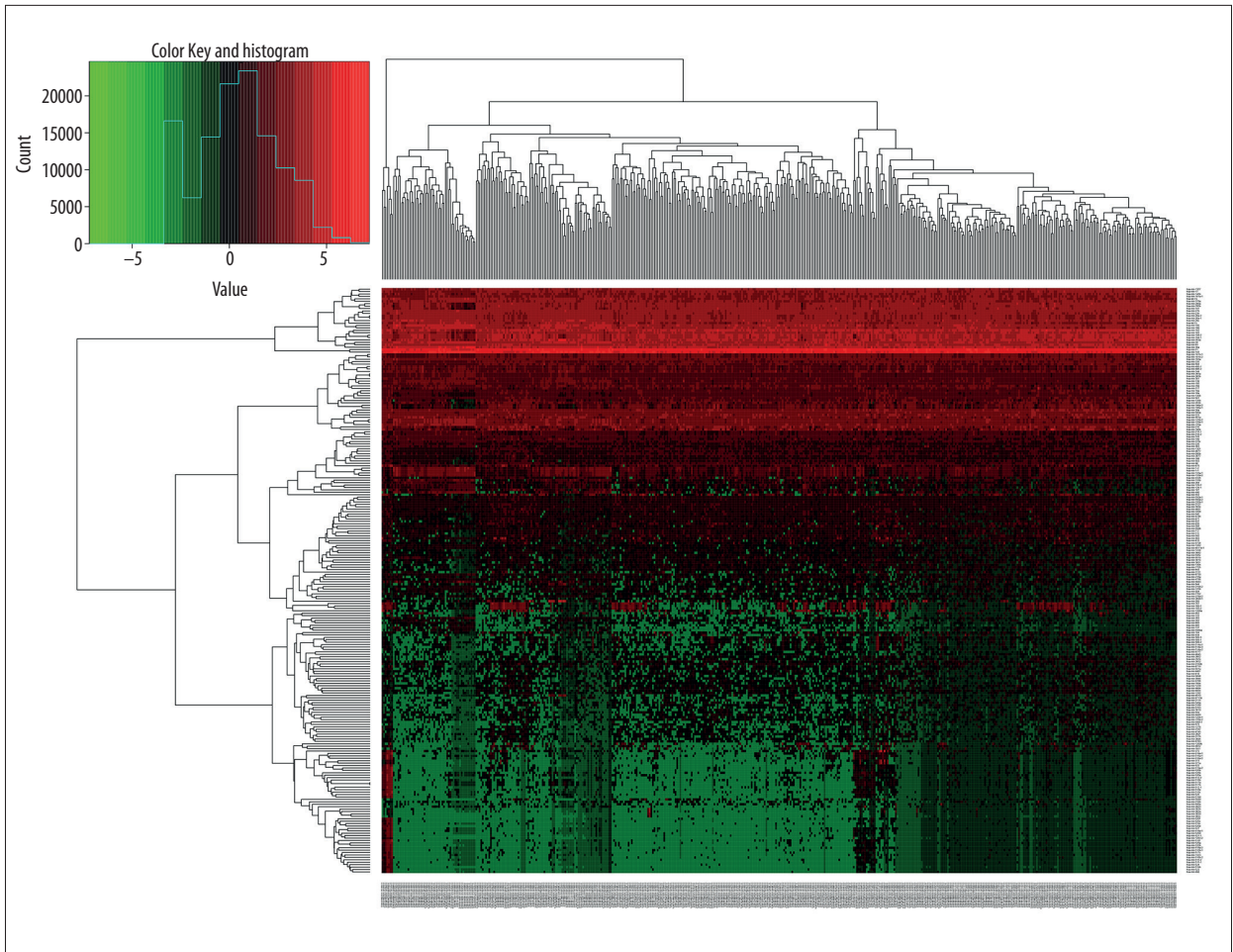
None.

## Supplementary Data

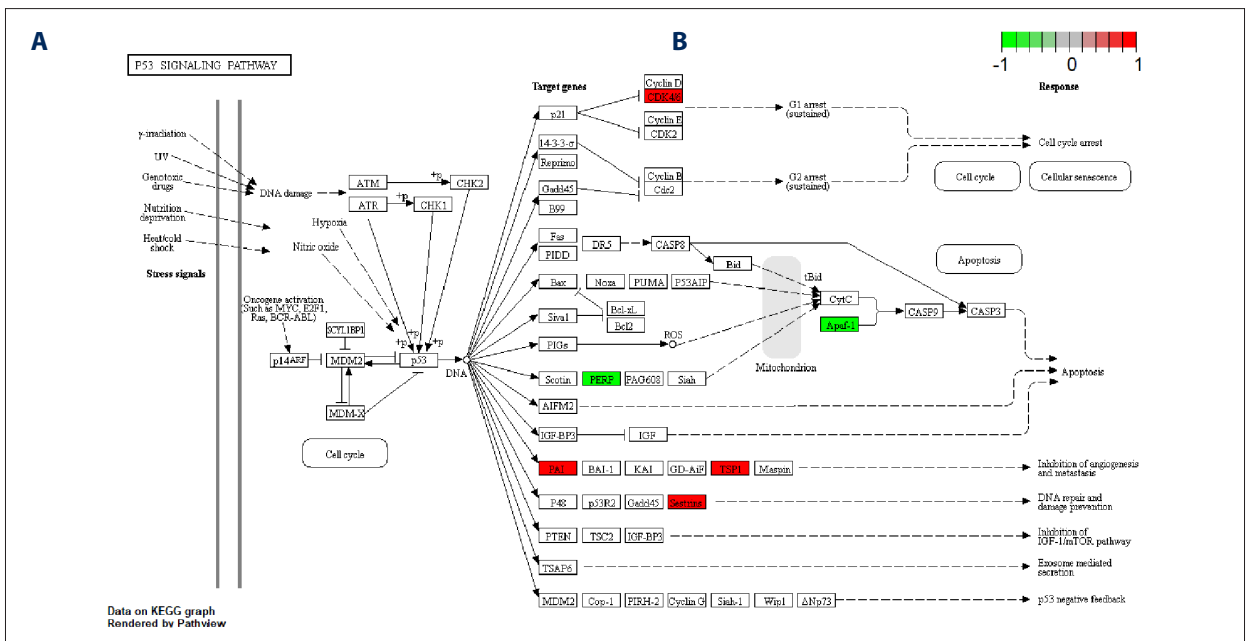
Supplementary Tables 1–6 available from the corresponding author on request.



**Supplementary Figure 1.** (A) The intersection of targeting mRNAs and DEmRNAs. (B) The intersection of targeting miRNAs and DEmiRNAs. mRNA – messenger RNA; DE – differentially expressed; miRNA – microRNA.



Supplementary Figure 2. Heatmap of differentially expressed miRNAs in gastric cancer on TCGA. miRNA – microRNA; TCGA – The Cancer Genome Atlas





22. Sun H, Xi P, Sun Z et al: Circ-SFMBT2 promotes the proliferation of gastric cancer cells through sponging miR-182-5p to enhance CREB1 expression. *Cancer Manag Res*, 2018; 10: 5725–34
23. Li Y, Chen S, Shan Z et al: miR-182-5p improves the viability, mitosis, migration, and invasion ability of human gastric cancer cells by down-regulating RAB27A. *Biosci Rep*, 2017; 37(3): pii: BSR20170136
24. Wang J, Li L, Jiang M, Li Y: MicroRNA-195 inhibits human gastric cancer by directly targeting basic fibroblast growth factor. *Clin Translat Oncol*, 2017; 19(11): 1320–28
25. Ye R, Wei B, Li S et al: Expression of miR-195 is associated with chemotherapy sensitivity of cisplatin and clinical prognosis in gastric cancer. *Oncotarget*, 2017; 8(57): 97260–72
26. Ye B, Jiang LL, Xu HT et al: Expression of PI3K/AKT pathway in gastric cancer and its blockade suppresses tumor growth and metastasis. *Int J Immunopathol Pharmacol*, 2012; 25(3): 627–36
27. Yang Q, Jiang W, Hou P: Emerging role of PI3K/AKT in tumor-related epigenetic regulation. *Semin Cancer Biol*, 2019 [Epub ahead of print]
28. Harris SL, Levine AJ: The p53 pathway: Positive and negative feedback loops. *Oncogene*, 2005; 24(17): 2899–908
29. Wei GH, Wang X: LncRNA MEG3 inhibit proliferation and metastasis of gastric cancer via p53 signaling pathway. *Eur Rev Med Pharmacol Sci*, 2017; 21(17): 3850–56
30. Naumov GN, Bender E, Zurakowski D et al: A model of human tumor dormancy: An angiogenic switch from the nonangiogenic phenotype. *J Natl Cancer Inst*, 2006; 98(5): 316–25
31. Jeanne A, Schneider C, Martiny L, Dedieu S: Original insights on thrombospondin-1-related antireceptor strategies in cancer. *Front Pharmacol*, 2015; 6: 252
32. Tigan AS, Bellutti F, Kollmann K et al: CDK6-a review of the past and a glimpse into the future: From cell-cycle control to transcriptional regulation. *Oncogene*, 2016; 35(24): 3083–91
33. Xue M, Li G, Fang X et al: hsa\_circ\_0081143 promotes cisplatin resistance in gastric cancer by targeting miR-646/CDK6 pathway. *Cancer Cell Int*, 2019; 19: 25
34. Pavon MA, Arroyo-Solera I, Cespedes MV et al: uPA/uPAR and SERPINE1 in head and neck cancer: Role in tumor resistance, metastasis, prognosis and therapy. *Oncotarget*, 2016; 7(35): 57351–66
35. Vander Ark A, Cao J, Li X: TGF-beta receptors: In and beyond TGF-beta signaling. *Cell Signal*, 2018; 52: 112–20